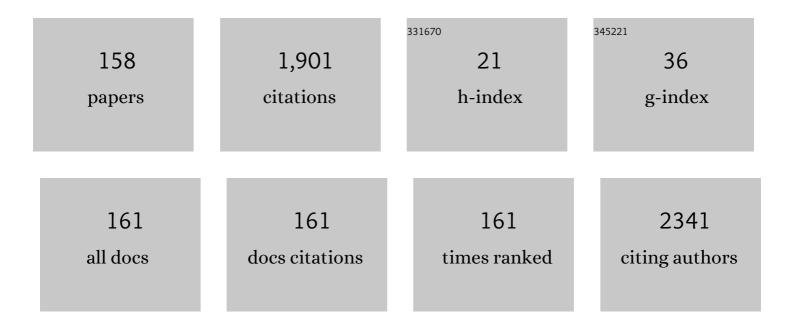
Benilde Costa

List of Publications by Year in descending order

Source: https://exaly.com/author-pdf/6576582/publications.pdf Version: 2024-02-01



#	Article	IF	CITATIONS
1	Fe2O3/aluminum thermite reaction intermediate and final products characterization. Materials Science & Engineering A: Structural Materials: Properties, Microstructure and Processing, 2007, 465, 199-210.	5.6	110
2	In Situ Synthesis of Magnetite Nanoparticles in Carrageenan Gels. Biomacromolecules, 2007, 8, 2350-2357.	5.4	107
3	Size-controlled synthesis of superparamagnetic iron oxide nanoparticles and their surface coating by gold for biomedical applications. Journal of Magnetism and Magnetic Materials, 2012, 324, 3997-4005.	2.3	106
4	Rhombohedral-to-orthorhombic transition and multiferroic properties of Dy-substituted BiFeO3. Journal of Applied Physics, 2010, 108, .	2.5	86
5	Distinct microbial populations are tightly linked to the profile of dissolved iron in the methanic sediments of the Helgoland mud area, North Sea. Frontiers in Microbiology, 2015, 06, 365.	3.5	72
6	Effect of Fe-doping on the structure and magnetoelectric properties of (Ba _{0.85} Ca _{0.15})(Ti _{0.9} Zr _{0.1})O ₃ synthesized by a chemical route. Journal of Materials Chemistry C, 2016, 4, 1066-1079.	5.5	60
7	Phase investigation of as-prepared iron oxide/hydroxide produced by sol–gel synthesis. Materials Letters, 2005, 59, 859-863.	2.6	50
8	Biofunctionalized magnetic hydrogel nanospheres of magnetite and $\hat{l}^{\rm o}$ -carrageenan. Nanotechnology, 2009, 20, 355602.	2.6	45
9	Structural, ferroelectric and magnetic properties of Bi _{0.85} Sm _{0.15} FeO ₃ perovskite. Crystal Research and Technology, 2011, 46, 238-242.	1.3	43
10	Electrical conductivity and dielectric properties of Sr doped M-type barium hexaferrite BaFe ₁₂ O ₁₉ . RSC Advances, 2021, 11, 1531-1542.	3.6	37
11	Structural, optical and dielectric properties of Cu _{1.5} Mn _{1.5} O ₄ spinel nanoparticles. RSC Advances, 2020, 10, 42542-42556.	3.6	35
12	Effects of oxygen deficiency on the transport and dielectric properties of NdSrNbO. Journal of Physics and Chemistry of Solids, 2018, 117, 1-12.	4.0	33
13	Magnetic ordering above room temperature in the sigma-phase of Fe66V34. Journal of Magnetism and Magnetic Materials, 2009, 321, 2160-2165.	2.3	31
14	BiFeO3 ceramic matrix with Bi2O3 or PbO added: Mössbauer, Raman and dielectric spectroscopy studies. Physica B: Condensed Matter, 2011, 406, 2532-2539.	2.7	31
15	Supercritically dried superparamagnetic mesoporous silica nanoparticles for cancer theranostics. Materials Science and Engineering C, 2020, 115, 111124.	7.3	28
16	Infrared and Mössbauer studies of iron in aluminosilicate glasses. Journal of Non-Crystalline Solids, 2001, 293-295, 534-538.	3.1	26
17	Mechanically induced phase transformations of the sigma phase of nanograined and of coarse-grained near-equiatomic FeCr alloys. Journal of Alloys and Compounds, 2006, 424, 131-140.	5.5	23
18	Structural, morphological, Raman and ac electrical properties of the multiferroic sol-gel made Bi0.8Er0.1Ba0.1Fe0.96Cr0.02Co0.02O3 material. Journal of Alloys and Compounds, 2019, 775, 304-315.	5.5	23

#	Article	IF	CITATIONS
19	Magnetic properties of a nanocrystalline σ-FeCr alloy. Journal of Physics Condensed Matter, 2005, 17, 2985-2992.	1.8	22
20	Controlled phase formation of nanocrystalline iron oxides/hydroxides in solution – An insight on the phase transformation mechanisms. Materials Chemistry and Physics, 2015, 163, 88-98.	4.0	22
21	Intermediate phases of the α-Ï f phase transition in the Fe-Cr system. Physical Review B, 1993, 47, 12257-12259.	3.2	21
22	Development and characterization of iron-pectin beads as a novel system for iron delivery to intestinal cells. Colloids and Surfaces B: Biointerfaces, 2018, 170, 538-543.	5.0	21
23	Structural, electric and dielectric properties of Ni0.5Zn0.5FeCoO4 ferrite prepared by sol-gel. Journal of Magnetism and Magnetic Materials, 2020, 499, 166243.	2.3	21
24	Study of Alpha-Sigma Phase Transformation in Mechanically Alloyed Fe-Cr-Sn Alloys. Physica Status Solidi A, 2001, 183, 235-250.	1.7	20
25	Gelatin-assisted sol–gel derived TiO2 microspheres for hydrogen storage. International Journal of Hydrogen Energy, 2015, 40, 4945-4950.	7.1	19
26	Development of a biocompatible magnetic nanofluid by incorporating SPIONs in Amazonian oils. Spectrochimica Acta - Part A: Molecular and Biomolecular Spectroscopy, 2017, 172, 135-146.	3.9	18
27	The Debye temperature of the Fe–Cr sigma-phase alloys. Journal of Physics Condensed Matter, 2005, 17, 6889-6893.	1.8	17
28	Design of multifunctional magnetic hybrid silica aerogels with improved properties. Microporous and Mesoporous Materials, 2016, 232, 227-237.	4.4	16
29	Disorder of Fe(2)O5 bipyramids and spin-phonon coupling in SrFe12O19 nanoparticles. Ceramics International, 2019, 45, 13571-13574.	4.8	16
30	Effect of annealing temperature on structural, morphological and dielectric properties of La0.8Ba0.1Ce0.1FeO3 perovskite. Journal of Materials Science: Materials in Electronics, 2020, 31, 16220-16234.	2.2	16
31	Effect of Bi-substitution into the A-site of multiferroic La _{0.8} Ca _{0.2} FeO ₃ on structural, electrical and dielectric properties. RSC Advances, 2020, 10, 16132-16146.	3.6	16
32	Mössbauer studies of phase separation in nanocrystalline Fe0.55â^'xCr0.45Snx alloys prepared by mechanical alloying. Journal of Alloys and Compounds, 2003, 350, 36-46.	5.5	15
33	Characterization of iron(III) oxide/hydroxide nanostructured materials produced by sol–gel technology based on the Fe(NO3)3·9H2O–C2H5OH–CH3CHCH2O system. Materials Chemistry and Physics, 2011, 130, 548-560.	4.0	15
34	Mechanical Alloying of Fe-Cu Alloys from As-Received and Premilled Elemental Powder Mixtures. Key Engineering Materials, 2002, 230-232, 631-634.	0.4	14
35	Mössbauer spectrometry of near equiatomic Fe–Cr alloys: Influence of preparation method. Journal of Alloys and Compounds, 2007, 434-435, 584-586.	5.5	14
36	Effect of activating flux and shielding gas on microstructure of TIG welds in austenitic stainless steel. Science and Technology of Welding and Joining, 2009, 14, 315-320.	3.1	14

#	Article	IF	CITATIONS
37	Debye temperature of disordered bcc-Fe–Cr alloys. Journal of Physics Condensed Matter, 2010, 22, 055402.	1.8	14
38	Sol–gel synthesis of iron(III) oxyhydroxide nanostructured monoliths using Fe(NO3)3A·9H2O/CH3CH2OH/NH4OH ternary system. Journal of Physics and Chemistry of Solids, 2011, 72, 678-684.	4.0	14
39	Structural and Magnetic Studies of Annealed Iron Oxide Nanoparticles. Journal of Superconductivity and Novel Magnetism, 2020, 33, 3249-3261.	1.8	14
40	Structural study and large magnetocaloric entropy change at room temperature of La _{1â^'x} â—i _x MnO ₃ compounds. RSC Advances, 2020, 10, 8352-8363.	3.6	14
41	Influence of Al3+ substituted cobalt nano-ferrite on structural, morphological and magnetic properties. Journal of Alloys and Compounds, 2021, 854, 156968.	5.5	13
42	Crystal structure of hydrated diphenylguanidinium hexafluoroferrate (III). Journal of Fluorine Chemistry, 2000, 106, 77-81.	1.7	12
43	Highly fluorescent and superparamagnetic nanosystem for biomedical applications. Nanotechnology, 2017, 28, 285704.	2.6	12
44	Biocompatible and high-magnetically responsive iron oxide nanoparticles for protein loading. Journal of Physics and Chemistry of Solids, 2019, 134, 273-285.	4.0	12
45	Effect of controlled crystallization on polaronic transport in phosphateâ€based glassâ€ceramics. International Journal of Applied Glass Science, 2020, 11, 97-111.	2.0	12
46	High electrical conductivity at room temperature of MnCo2O4 cobaltite spinel prepared by sol–gel method. Journal of Materials Science: Materials in Electronics, 2021, 32, 1221-1232.	2.2	12
47	Magnetic properties of coarse-grained and nanocrystalline Fe–Cr–Sn alloys. Journal of Alloys and Compounds, 2000, 308, 49-55.	5.5	11
48	On the Debye temperature in sigma-phase Fe–V alloys. Intermetallics, 2010, 18, 1695-1698.	3.9	11
49	Superparamagnetic core-shell nanocomplexes doped with Yb 3+ : Er 3+ /Ho 3+ rare-earths for upconversion fluorescence. Materials and Design, 2017, 130, 263-274.	7.0	11
50	Investigating the structural, morphological, dielectric and electric properties of the multiferroic (La0.8Ca0.2)0.9Bi0.1FeO3 material. Chemical Physics Letters, 2019, 731, 136588.	2.6	11
51	Effect of synthesis route on structural, morphological, Raman, dielectric, and electric properties of La0.8Ba0.1Bi0.1FeO3. Journal of Materials Science: Materials in Electronics, 2020, 31, 3197-3214.	2.2	11
52	Investigation of temperature and frequency dependence of the dielectric properties of multiferroic (La _{0.8} Ca _{0.2}) _{0.4} Bi _{0.6} FeO ₃ nanoparticles for energy storage application. RSC Advances, 2022, 12, 6907-6917.	3.6	11
53	Kinetics of σ-phase formation in equiatomic cold-rolled Fe–V alloys. Materials Chemistry and Physics, 2013, 143, 19-25.	4.0	10
54	Magneto-Transport Properties of the Ag Doping Sr Site in La0.57Nd0.1Sr0.33â^'xAgxMnO3 (0.00 and 0.15) Manganites. Journal of Low Temperature Physics, 2020, 200, 131-141.	1.4	10

#	Article	IF	CITATIONS
55	Investigation of the magnetocaloric effect and the critical behavior of the interacting superparamagnetic nanoparticles of La0.8Sr0.15Na0.05MnO3. Journal of Alloys and Compounds, 2022, 890, 161739.	5.5	10
56	On the Role of Tin Solubility in the Precipitation of the Sigma-Phase in Fe–Cr–Sn Alloys. Physica Status Solidi A, 1997, 164, 687-697.	1.7	9
57	Phase transformations of l̃ f -FeCr induced by ball milling. Hyperfine Interactions, 2005, 165, 107-112.	0.5	9
58	Kinetics of the sigma-to-alpha phase transformation caused by ball milling in near equiatomicFeâ~Cralloys. Physical Review B, 2006, 73, .	3.2	9
59	Delayed electron capture and formation in ZnSe. Physica B: Condensed Matter, 2009, 404, 888-891.	2.7	9
60	Synthesis, structure and magnetic properties of multipod-shaped cobalt ferrite nanocrystals. New Journal of Chemistry, 2019, 43, 10259-10269.	2.8	9
61	Structural, Morphological, Raman, and Mössbauer Studies on (La0.8Ca0.2)1â^'xBixFeO3 (x = 0.0, 0.1, and) Tj ET	Qq1 1 0.7	784314 rgBT
62	Formation stages of bcc (Fe44Co44)Sn12 extended solid solution by mechanical alloying. Journal of Alloys and Compounds, 2014, 615, S559-S563.	5.5	8
63	B2 long-range order in mechanically alloyed Fe53.3â^'0.6x Co46.7â^'0.4x Sn x (2Ââ‰ÂxÂâ‰Â26) annealed at moderate temperatures. Journal of Materials Science, 2016, 51, 5775-5790.	3.7	8
64	Study of structural, morphological, Mössbauer and dielectric properties of NiFeCoO4 prepared by a sol gel method. Journal of Sol-Gel Science and Technology, 2021, 98, 364-375.	2.4	8
65	Recycling of mining waste in the synthesis of magnetic nanomaterials for removal of nitrophenol and polycyclic aromatic hydrocarbons. Chemical Physics Letters, 2021, 771, 138482.	2.6	8
66	Structural, morphological, Raman, dielectric and electrical properties of La _{1â^²2<i>x</i>} Ba _{<i>x</i>} Bi _{<i>x</i>} FeO ₃ (0.00 ≤i>x	›) ₿jÆTQq	0 &0 rgBT /O
67	Evolution of a FeV sigma phase ball-milled in a mixture of argon and air. Hyperfine Interactions, 2008, 183, 67-73.	0.5	7
68	Order-disorder phenomena from X-ray diffraction in FeCo alloys annealed and ground at high energy. Powder Diffraction, 2011, 26, 267-272.	0.2	7
69	Mössbauer studies of Haltern 70 amphorae from Castro do Vieito, North of Portugal, and of amphora sherds from kilns in the Roman provinces Hispania Baetica and Lusitania. Hyperfine Interactions, 2011, 202, 81-87.	0.5	7
70	Mechanosynthesis of supersaturated solid solutions of Sn in near-equiatomic bcc FeCo. Journal of Alloys and Compounds, 2012, 536, S31-S34.	5.5	7
71	Synthesis and study of structural, optical, and electrical properties of nontoxic and earth-abundant Na2ZnSnS4 material. Journal of Materials Science: Materials in Electronics, 2020, 31, 18858-18869.	2.2	7
72	Synthesis and investigation of oxygen deficiency effect on electric properties of La0.75Ba0.10Sr0.15FeO2.875-δ (δ = 0.00, 0.125 and 0.25) ferrites. Journal of Materials Science: Materia Electronics, 2021, 32, 13000-13013.	alsin	7

#	Article	IF	CITATIONS
73	Structural, dielectric relaxation and magnetic features of the (La0.8Ca0.2)0.9Bi0.1Fe1â^'yTiyO3 (y = 0.0) Tj l	ETQg1 1	0.784314 rg
74	Novel Kevlar® pulp-reinforced alumina-silica aerogel composites for thermal insulation at high temperature. Journal of Sol-Gel Science and Technology, 2022, 101, 87-102.	2.4	7
75	Magnetic and Transport Studies of the α—σ Transformation in Fe54Cr46 and Fe52Cr46Sn2 Alloys: Kinetics of σ Phase Formation. Physica Status Solidi A, 1997, 161, 349-360.	1.7	6
76	The Influence of Pre-Milling on the Microstructural Evolution During Mechanical Alloying of a Fe ₅₀ Cu ₅₀ Alloy Journal of Metastable and Nanocrystalline Materials, 2003, 18, 49-0.	0.1	6
77	The Debye temperature of a nanocrystalline Â-Fe55.4Cr44.6alloy. Journal of Physics Condensed Matter, 2004, 16, L343-L346.	1.8	6
78	The Debye temperature of quasi-equi-atomic α-Fe–Cr alloys. Journal of Physics Condensed Matter, 2006, 18, 10899-10903.	1.8	6
79	Anomalous behaviour of the Debye temperature in Fe-rich Fe–Cr alloys. Journal of Alloys and Compounds, 2010, 492, L1-L4.	5.5	6
80	Cellulose/iron oxide hybrids as multifunctional pigments in thermoplastic starch based materials. Cellulose, 2013, 20, 861-871.	4.9	6
81	Synthesis and study of the structural and dielectric properties of La0.67Ca0.2Ba0.13Fe1â^'xMnxO3 ferrites (x = 0, 0.03 and 0.06). Journal of Materials Science: Materials in Electronics, 2021, 32, 7926-794	2. ^{2.2}	6
82	Investigation of Cr substitution effect on the evolution of La0.67Ca0.2Ba0.13Fe1â^'xCrxO3 (x = 0 and C electrical properties under frequency and temperature variation. European Physical Journal Plus, 2021, 136, 1.	0.03) 2.6	6
83	Effect of the annealing temperature and of Bi substitution on the structural and magnetic behaviors of double-doping (Bi/La, Ca) (La0.8Ca0.2)1â^'xBixFeO3 compounds. New Journal of Chemistry, 2020, 44, 9813-9821.	2.8	6
84	Characterization of mechanically alloyed Fe–Cr–Sn alloys. Journal of Materials Processing Technology, 1999, 92-93, 395-400.	6.3	5
85	Low temperature resistivity studies of Fe–Cr–Sn alloys in alpha and sigma phases. Journal of Alloys and Compounds, 2000, 297, 15-20.	5.5	5
86	Investigation of a Cr42.2Fe57.8alloy prepared by mechanical alloying. Journal of Physics Condensed Matter, 2006, 18, 3263-3276.	1.8	5
87	Partial amorphization of an α-FeCr alloy by ball-milling. Hyperfine Interactions, 2008, 183, 109-115.	0.5	5
88	Synthesis, structure and magnetic behaviour of mixed metal leucophosphite. Journal of Solid State Chemistry, 2008, 181, 1330-1336.	2.9	5
89	The effect of oxygen on ball milling of a near-equiatomic FeV sigma phase. Journal of Applied Physics, 2008, 104, 084315.	2.5	5
90	X-ray compositional microanalysis and diffraction studies of Haltern 70 amphorae sherds. X-Ray Spectrometry, 2012, 41, 69-74.	1.4	5

#	Article	IF	CITATIONS
91	57FE Mössbauer spectroscopy studies of Tektites from Khon Kaen, Ne Thailand. Hyperfine Interactions, 2014, 224, 51-56.	0.5	5
92	Debye temperature of nanocrystalline Fe–Cr alloys obtained by mechanical alloying. Journal of Alloys and Compounds, 2015, 649, 1246-1252.	5.5	5
93	Synthesis and physicochemical characterizations of a new valence-mixed pyrophosphate: Cu 0.5 Zn 0.5 Fe 2 (P 2 O 7) 2. Journal of Physics and Chemistry of Solids, 2018, 119, 122-125.	4.0	5
94	Synthesis and physicochemical characterization of a new mixed-valence IronIII-ZincII diphosphate: Zn2+Fe3+2(P2O7)2. Materials Chemistry and Physics, 2018, 216, 22-27.	4.0	5
95	Design and development a novel uranyl sensor based on FePt/ZnIn2S4 core-shell semiconductor nanostructures. Arabian Journal of Chemistry, 2020, 13, 1429-1439.	4.9	5
96	Assessment of structural, optical, magnetic, magnetocaloric properties and critical phenomena of La0.57Nd0.1Sr0.18Ag0.15MnO3 system at room temperature. Journal of Materials Science: Materials in Electronics, 2020, 31, 11983-11996.	2.2	5
97	57Fe Mössbauer Studies in Mo–Fe Supported Catalysts. Hyperfine Interactions, 2001, 136, 9-16.	0.5	4
98	Structural analysis and 57Fe Mössbauer spectrometry of Zr6FeSn2 and related compounds. Journal of Alloys and Compounds, 2007, 438, 88-91.	5.5	4
99	Mössbauer spectrometry of near equiatomic Fe–Cr alloys: Phase separation at high temperature?. Journal of Alloys and Compounds, 2007, 434-435, 587-589.	5.5	4
100	Superferromagnetism in mechanically alloyed fcc Fe ₂₃ Cu ₇₇ with bimodal cluster size distribution. Journal of Physics Condensed Matter, 2009, 21, 046003.	1.8	4
101	The effect of composition and temperature on the amount and type of nanoferrite particles inserted in Fe2O3–ZnO–MgO–SiO2 glass–ceramics. Journal of Non-Crystalline Solids, 2011, 357, 3722-3725.	3.1	4
102	Solâ€gel synthesis and washing of amorphous gâ€FeO(OH) xerogels. Materialwissenschaft Und Werkstofftechnik, 2012, 43, 427-434.	0.9	4
103	57Fe Mössbauer, SEM/EDX, p-XRF and μ-XRF studies on a Dutch painting. Hyperfine Interactions, 2016, 237, 1.	0.5	4
104	Novel synthesis and application of FePt/CuInS2 magneto-optical core-shell nanostructures in copper ions sensing. Sensors and Actuators B: Chemical, 2018, 254, 448-456.	7.8	4
105	Airborne environmental fine particles induce intense inflammatory response regardless of the absence of heavy metal elements. Ecotoxicology and Environmental Safety, 2020, 195, 110500.	6.0	4
106	Assessment of the critical behavior in the multiferroic Bi0.8Ba0.1Er0.1Fe0.96Cr0.02Co0.02O3 material, multi-substitution effect on magnetic and M¶ssbauer properties. Journal of Magnetism and Magnetic Materials, 2021, 524, 167640.	2.3	4
107	Synthesis and physico-chemical characterization of Bi-doped Cobalt ferrite nanoparticles: cytotoxic effects against breast and prostate cancer cell lines. European Physical Journal Plus, 2022, 137, .	2.6	4
108	Hydrogen effect on the sigma-phase in Fe53.8Cr46.2. Journal of Alloys and Compounds, 2009, 467, 182-186.	5.5	3

#	Article	IF	CITATIONS
109	Ball-milling in vacuum of $\hat{l}\pm$ and $\ddot{l}f$ phases of near-equiatomic FeCr alloys. Journal of Alloys and Compounds, 2009, 483, 70-73.	5.5	3
110	Mössbauer study of Haltern 70 amphora sherds from Castro do Vieito, North of Portugal. Journal of Physics: Conference Series, 2010, 217, 012060.	0.4	3
111	Study of a sigma-phase formation in an equiatomic Fe-V alloy. Journal of Physics: Conference Series, 2010, 217, 012077.	0.4	3
112	Comparison of disorder induced by annealing and quench and by ballâ€milling in B2 FeCo. Physica Status Solidi C: Current Topics in Solid State Physics, 2011, 8, 3087-3090.	0.8	3
113	Mechanically Driven Dissolution of Sn in Near-Equiatomic Bcc FeCo. Solid State Phenomena, 2012, 194, 187-193.	0.3	3
114	Klimt artwork: material investigation by backscattering Fe-57 Mössbauer and Raman spectroscopy. Hyperfine Interactions, 2014, 226, 621-627.	0.5	3
115	Backscattering Mössbauer MIMOS II and XRF studies on tektites from different strewn fields. Hyperfine Interactions, 2014, 226, 613-619.	0.5	3
116	Nanostructured Titania Photoanodes for Dye Solar Cells. Materials Today: Proceedings, 2015, 2, 141-146.	1.8	3
117	Synthesis, Structural Studies, and Magnetic Properties of a New Mixed-Valence Diphosphate: Zn2+5Fe3+2(P2O7)4. Journal of Superconductivity and Novel Magnetism, 2020, 33, 1007-1012.	1.8	3
118	Influence of oxygen deficiency on optical and dielectric properties of La0.75Ba0.10Sr0.15FeO2.875-δ compounds. Chemical Physics Letters, 2020, 741, 137106.	2.6	3
119	A technical note on the phase transformation in furnace container material after a periodic thermo-chemical treatment. Journal of Materials Processing Technology, 2002, 122, 363-367.	6.3	2
120	Laser selectivity on cleaning museologic iron artefacts. , 2006, , .		2
121	Mössbauer spectroscopy and X-ray diffraction studies of ball-milling-induced transformations of a near-equiatomic FeV sigma phase: Influence of oxygen. Nuclear Instruments and Methods in Physics Research, Section A: Accelerators, Spectrometers, Detectors and Associated Equipment, 2007, 580, 404-407.	1.6	2
122	Study of Hydrogen in Hf ₇ Ni ₁₀ Combined with TiV _{0.8} Cr _{1.2} by PAC. Solid State Phenomena, 0, 170, 293-297.	0.3	2
123	The influence of the heat treatment temperature in the magnetic characteristics of a SiO2–Li2O–Fe2O3 glass prepared by sol-gel. Journal of Non-Crystalline Solids, 2014, 391, 32-38.	3.1	2
124	Mössbauer investigation of novel pentadentate schiff base complexes. Hyperfine Interactions, 2016, 237, 1.	0.5	2
125	Mössbauer and XRD studies of Roman amphorae buried in the sea for two millennia. Hyperfine Interactions, 2016, 237, 1.	0.5	2
126	Klimt artwork (Part II): material investigation by backscattering Fe-57 Mössbauer- and Raman- spectroscopy, SEM and p-XRF. Hyperfine Interactions, 2016, 237, 1.	0.5	2

#	Article	IF	CITATIONS
127	Klimt artwork: red-pigment material investigation by backscattering Fe-57 Mössbauer spectroscopy, SEM and p-XRF. Science and Technology of Archaeological Research, 2017, 3, 450-455.	2.4	2
128	Magnetic Studies on New Mixed-Valence Phosphates Zn2+Fe 2 3 + \$_{2}^{3+}\$ (P2O7)2 and Zn. Journal of Superconductivity and Novel Magnetism, 2019, 32, 1377-1382.	1.8	2
129	Influence of Non-magnetic Ti4+ Ion Doping at Mn Site on Structural, Magnetic, and Magnetocaloric Properties of La0.5Pr0.2Sr0.3Mn1â``xTixO3 Manganites (x = 0.0 and 0.1). Journal of Superconductivity and Novel Magnetism, 2019, 32, 1653-1662.	1.8	2
130	Assessment of nanostructure, optical, dielectric and modulus response by Bi substitution in La1â^'xBixNi0.5Ti0.5O3 (x = 0.0–0.2) system. European Physical Journal Plus, 2021, 136, 1.	2.6	2
131	57Fe Mössbauer Analysis of Meteorites and Tektites. Minerals (Basel, Switzerland), 2021, 11, 628.	2.0	2
132	First 119Sn Mössbauer-effect study of the σ-phase in the Fe-Cr system. Journal of Magnetism and Magnetic Materials, 1992, 115, 307-310.	2.3	1
133	Elevated temperature failure of heat treatment furnace containers. Materials Science and Technology, 2000, 16, 436-441.	1.6	1
134	Magnetic and transport studies of Ïf-phase Fe50V50 alloys with different thermal history. Journal of Non-Crystalline Solids, 2008, 354, 5287-5289.	3.1	1
135	Development of High Curie Temperature Ferroelectric xBi(Sc _{0.5} ,Yb _{0.5})O ₃ –(1-x)PbTiO ₃ Single Crystals. Ferroelectrics, 2013, 447, 33-39.	0.6	1
136	North West Africa stony meteorite: a case study. Hyperfine Interactions, 2020, 241, 1.	0.5	1
137	Specific features of structural, magnetic, Raman and Mössbauer: Properties of La0.57Nd0.10Sr0.18Ag0.15FeO3 ferrite nanoparticules. Journal of Molecular Structure, 2021, 1238, 130344.	3.6	1
138	X-Ray Fluorescence Spectrometry With Gas Proportional Scintillation Counters. Advances in X-ray Analysis, 1987, 31, 445-448.	0.0	1
139	Effect of the Multiple Electrodes TIG Welding Process on the Metallurgical Properties of Welds in Austenitic Stainless Steels. Key Engineering Materials, 2002, 230-232, 140-143.	0.4	Ο
140	Synthesis, Magnetic and Mössbauer Studies of Mechanically Alloyed Fe _{0.63} Si _{0.37} Alloys. Materials Science Forum, 2006, 514-516, 1265-1268.	0.3	0
141	X-ray diffraction and Mössbauer spectrometry studies of molecular iron compounds. Nuclear Instruments and Methods in Physics Research, Section A: Accelerators, Spectrometers, Detectors and Associated Equipment, 2007, 580, 408-411.	1.6	Ο
142	Ball Milling of the β-FeSi ₂ Phase. Materials Science Forum, 0, 587-588, 410-414.	0.3	0
143	Ball Milling of an Equiatomic <i>Ïf</i> -FeV Alloy in Vacuum. Journal of Nanoscience and Nanotechnology, 2010, 10, 2850-2852.	0.9	0
144	Magnetic study of amorphization of ball-milled FeCr alloys. Journal of Physics: Conference Series, 2010, 200, 082017.	0.4	0

#	Article	IF	CITATIONS
145	Long ball-milling of bcc-FeCr at different injected powers: Amorphization and partial crystallization. Journal of Physics: Conference Series, 2010, 217, 012103.	0.4	0
146	Long-time ball milling of FeCr. International Journal of Nanomanufacturing, 2010, 5, 10.	0.3	0
147	X-Ray Diffraction and Mössbauer Studies of Sigma-FeV Alloys Ball-Milled in Vacuum. Materials Science Forum, 2010, 636-637, 941-945.	0.3	0
148	Electric Properties of Single-Phased BiFeO ₃ Ceramics. Ferroelectrics, 2013, 452, 57-62.	0.6	0
149	Mössbauer studies of a martensitic transformation and of cryogenic treatments of a D2 tool steel. Hyperfine Interactions, 2013, 219, 135-139.	0.5	0
150	Perovskite xBilnO3-(1â^'x)PbTiO3Crystals. Ferroelectrics, 2013, 457, 39-43.	0.6	0
151	Iron(III) Complexes on a Dendrimeric Basis and Various Amine Core Investigated by Mössbauer Spectroscopy. Journal of Physics: Conference Series, 2014, 534, 012003.	0.4	0
152	Mössbauer spectroscopy and X-ray fluorescence studies on sediments from the methanic zone of the Helgoland mud area, North Sea. Hyperfine Interactions, 2016, 237, 1.	0.5	0
153	Mechanosynthesis of bcc alloys from Fe50â^'y/2Co50â^'y/2Sn y mixtures (2 â‰ኳ â‰ኳ3) and B2 ordering by annealing at modest temperatures. Hyperfine Interactions, 2017, 238, 1.	0.5	0
154	Study of the magneto transport properties at room temperature in lacunary ceramics La0,8-xâ–¡xNa0,2-xâ–¡xMnO3 in site A. Journal of Superconductivity and Novel Magnetism, 2020, 33, 313-322.	1.8	0
155	Analysis of the electrical transport, conductivity, and dielectric relaxation behavior of La0.75 Ba0.10 Sr0.15 Fe O2.875-δ (δ = 0.375 and 0.50) brownmillerite oxides. Journal of Materials Science: Materials in Electronics, 2021, 32, 21897-21908.	2.2	0
156	Study of the influence of 2.5% Mg2+ insertion in the B-site of La0.8Ca0.1Pb0.1FeO3 on its structural, electrical and dielectric properties. RSC Advances, 2021, 11, 33070-33080.	3.6	0
157	Mössbauer studies of Haltern 70 amphorae from Castro do Vieito, North of Portugal, and of amphora sherds from kilns in the Roman provinces Hispania Baetica and Lusitania. , 2011, , 81-87.		0
158	Window Area Effects in the Detector Efficiency for Source Excited EDXRF Geometries. Advances in X-ray Analysis, 1987, 31, 455-459.	0.0	0